processes

MDPI

Article

Collision Modes of Two Eccentric Compound Droplets

Khanh P. Nguyen [1] and Truong V. Vu [1,2,3,*]

[1] Faculty of Vehicle and Energy Engineering, Phenikaa University, Yen Nghia, Ha-Dong District, Hanoi 12116, Vietnam; khanh.nguyenphu@phenikaa-uni.edu.vn
[2] Faculty of Mechanical Engineering and Mechatronics, Phenikaa University, Yen Nghia, Ha-Dong District, Hanoi 12116, Vietnam
[3] Phenikaa Research and Technology Institute (PRATI), AA Green Phoenix Group, 167 Hoang Ngan, Hanoi 12116, Vietnam
* Correspondence: truong.vuvan@phenikaa-uni.edu.vn; Tel.: +84-0242-2180-336

Received: 23 April 2020; Accepted: 15 May 2020; Published: 18 May 2020

Abstract: A compound droplet with its single inner droplet appears in a broad range of applications and has received much attention in recent years. However, the role of the inner droplet location on the dynamical behaviors of the compound droplet is still not completely understood. Accordingly, the present study numerically deals with the eccentricity of the compound droplet affecting its colliding behaviors with the other droplet in a simple shear flow. The solving method is a front-tracking technique that treats the droplet interface as connected elements moving on a rectangular fixed grid. Initially, two compound droplets assumed circular are placed at a distance symmetrically to the domain center and they come into contact, because of the shear flow, when time progresses. During the collision process, the inner droplet that is initially located at a distance to its outer droplet center circulates around this center. It is found that this rotation also contributes to the formation of the collision modes including the reversing, passing-over and merging ones. Starting from a passing-over mode, a transition to a reversing mode or a merging mode can appear when the inner droplets, in terms of their centroids, are closer than their outer droplets. However, the location of the inner droplet within the outer droplet only has an effect when the value of the Capillary number Ca is varied from 0.01 to 0.08. For $Ca < 0.01$ corresponding to the merging mode and $Ca \geq 0.16$ corresponding to the passing-over mode, the inner droplet position has almost no impact on the collision behaviors of two compound droplets.

Keywords: eccentric compound droplet; collision; reversing; passing-over; merging

1. Introduction

In general, compound droplets exist in two types [1]. The first type of compound droplets is available with the outer interface partially enclosing its inner droplets [2]. Such a compound droplet is not considered in the present study. In the second type, a compound droplet consists of an outer interface (i.e., outer droplet) that completely encapsulates one or many inner droplets [3–5]. When the droplet is small, it is all called a "double or multiple emulsion droplet" [6]. The second type has shown its applications in many academic problems and industrial processes, for example, biotechnological processes [7], delivery of drugs [8] and some other applications [9]. In these processes and applications, a compound droplet can collide with one or many other ones and the dynamical behaviors of collisions have been classified into three main modes—reversing, passing-over and merging [10,11]. Before coming into contact with others, a compound droplet may carry one or many daughter droplets [6]. In this study, to simplify we pay attention to the compound droplets with one inner core (i.e., single-core compound droplets) that are suspended in a simple shear flow [11–13].

The dynamics of one single-core compound droplet in the simple shear flow has been investigated carefully for many years [14–17]. For example, Luo and his co-workers [17] considered an initially concentric droplet with its finite deformation caused by the shear of the continuous outer flow and the authors claimed that the compound droplets exhibit less deformation than those without any inner core (i.e., single-phase droplets). Chen et al. [15] numerically showed that the shear flow may cause the compound droplet to decompose into smaller droplets in three mechanisms—instability breakup, necking breakup and end-breakup. The transitions between the breakup and the finite deformation of the compound droplet were presented by Vu et al. [12]. However, as mentioned, these studies focused on the dynamical deformation and breakup of one droplet, which does not interact with any other. In addition, these works have not considered the effects of the compound droplet eccentricity. In a few other works, for example, References [18,19], the authors considered the role of the location of the inner droplet, that is, the eccentric compound droplet, in the dynamical behaviors of the droplet. Once again, these works [18,19] have not extended to the cases of binary droplets collisions as done in our present study.

Recently, few attempts have been made to investigate the dynamical interaction of two single-core compound droplets [10,11,20]. For instance, Liu and co-workers [11,20] considered two colliding modes (passing-over and reversing) of PVA (polyvinyl alcohol) solution/PS (polystyrene) solution/PVA solution droplets and compared with single-phase droplets. The authors found that the compound droplet moves in a similar trajectory but deforms differently as compared with the single-phase droplet. Revisiting this problem, our previous work [10] showed that, in addition to the passing-over and reversing modes, two compound droplets may become one as they are in contact with each other. This mode of collisions is merging. However, these works have not considered the effects of the position of the inner droplets on the collision behaviors of the droplets. This missing gap is the focus of our present work.

As aforementioned, in various applications of compound droplets including single-core compound droplets, droplet collisions may appear and the colliding behaviors are affected by the presence of the inner droplets [10,11]. Many applications indicated that when compound droplets are carried out by the continuous flow, their inner droplets are not concentric (e.g., Figure 1b in Reference [21], Figures 4 and 5 in References [22,23]) before or during the contact stage. Accordingly, the presence of the inner droplet and its position within its enclosing outer interface (i.e., droplet eccentricity) before the contacting stage should have an important role in the colliding behaviors. However, so far, such a detailed investigation has not been found. Hence, in this study, we consider eccentric compound droplets and investigate how the eccentricity leaves its impact on the dynamics of the collision. The rest of the paper is as follows. In the following section, we describe the numerical problem and its solving method. We then present the results of colliding behaviors under the influence of eccentricity. Finally, some concluding remarks are provided. To ease understanding, some animations of droplet collisions are also provided in the Supplementary Materials.

2. Numerical Problem and Method

In the present study, we deal with the collision of two compound droplets with only one core in each droplet (known as "single-core compound droplets"), which are suspended in a simple shear flow (Figure 1). As mentioned below, we focus on small-sized droplets with a little density difference and ignored buoyancy effects and thus the motions of the droplets during the collision are in the plane through their centers of mass [10,11]. Accordingly, a two-dimensional configuration to facilitate high-resolution computations with a reasonable computational cost, as considered in this study, can be accepted [10] even though three-dimensional simulations should be conducted. Initially, the compound droplets are placed symmetrically to the center (x_c, y_c) of the domain and the inner and outer droplets are circular and eccentric with the horizontal (ε_{x0}) and vertical (ε_{y0}) eccentricities defined as:

$$\varepsilon_{x0} = (x_{ci1} - x_{co1})\big|_{t=0} = 0.5(\Delta x_o - \Delta x_i)\big|_{t=0} \quad (1)$$

$$\varepsilon_{y0} = (y_{ci1} - y_{co1})\big|_{t=0} = 0.5(\Delta y_i - \Delta y_o)\big|_{t=0} \quad (2)$$

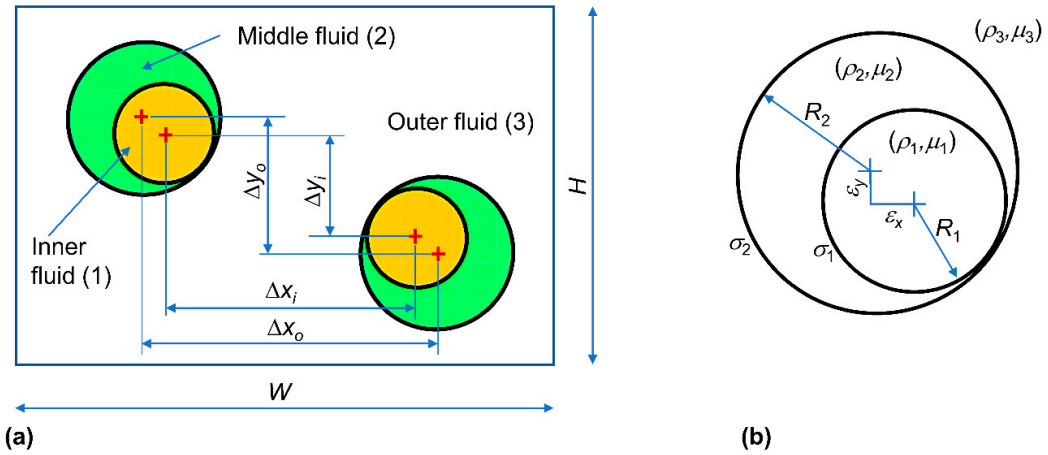

Figure 1. (**a**) The computational domain for the collision of two eccentric compound droplets with the left droplet denoted as "droplet 1" and the right one for "droplet 2." (**b**) The configuration of the compound droplet 1 [the droplet on the left side in (**a**)]. Each compound droplet consists of one inner droplet and is thus known as a "single-core compound droplet."

Here, Δx and Δy are the horizontal and vertical distances between two droplets with the subscripts i and o denoting respectively the inner and outer droplets. (x_{ci1}, y_{ci1}) and (x_{co1}, y_{co1}) are respectively the coordinates of the centroid of the inner droplet 1 and that of the outer droplet 1. Accordingly, for example, $\varepsilon_{x0} < 0$ and $\varepsilon_{y0} = 0$ correspond, in terms of droplet centroids, to the outer droplets closer than the inner droplets in the horizontal direction. The initial radii of the inner and outer droplets are R_1 and R_2, respectively. The inner droplet contains the inner fluid denoted by "fluid 1," the fluid in between the inner and outer interfaces, that is, the middle fluid, is called "fluid 2" and the rest is the outer, carrying fluid denoted by "fluid 3" Three fluids are assumed immiscible and each fluid has a constant density (denoted by ρ) and a constant viscosity (denoted by μ). The interfacial tension coefficients of the inner and outer droplet interfaces are respectively denoted by σ_1 and σ_2.

To handle the droplet interface and its movement, a front-tracking method [24,25] is used. The interface is modeled by a finite number of straight-line segments whose point coordinates $\mathbf{x}_f$ are updated by integrating the following equation:

$$\frac{d\mathbf{x}_f}{dt} = \mathbf{V}_n. \quad (3)$$

In Equation (3), the velocity $\mathbf{V}_n$ is interpolated from the nearest velocities solved from the following governing equations [10], on a background, rectangular and fixed grid:

$$\frac{\partial \rho u}{\partial t} + \frac{\partial \rho u^2}{\partial x} + \frac{\partial \rho uv}{\partial y} = -\frac{\partial p}{\partial x} + \frac{\partial}{\partial x} 2\mu \frac{\partial u}{\partial x} + \frac{\partial}{\partial y} \mu \left(\frac{\partial u}{\partial y} + \frac{\partial v}{\partial x} \right) + F_{bx} + F_{sx} \quad (4)$$

$$\frac{\partial \rho v}{\partial t} + \frac{\partial \rho uv}{\partial x} + \frac{\partial \rho v^2}{\partial y} = -\frac{\partial p}{\partial y} + \frac{\partial}{\partial x} \mu \left(\frac{\partial u}{\partial y} + \frac{\partial v}{\partial x} \right) + \frac{\partial}{\partial y} 2\mu \frac{\partial v}{\partial y} + F_{by} + F_{sy} \quad (5)$$

$$\frac{D\rho}{Dt} = \frac{D\mu}{Dt} = 0. \quad (6)$$

Equations (4)–(6) are for Newtonian and incompressible fluids with $\mathbf{u} = (u, v)$—velocity vector, p—pressure, t—time, $\mathbf{F}_b = (F_{bx}, F_{by})$—body force (e.g., gravity) and $\mathbf{F}_s = (F_{sx}, F_{sy})$—interfacial tension force defined as:

$$\mathbf{F}_s = \int_f \sigma\kappa\delta\left(\mathbf{x} - \mathbf{x}_f\right)\mathbf{n}_f dS. \quad (7)$$

In Equation (7), κ is the mean curvature, $\mathbf{n}_f$ is the unit vector normal to the droplet interface and the subscript f represents the interface. $\mathbf{n}_f$ points outward from the droplet. δ is the Dirac delta function. Like our previous paper [10], we consider small droplets with the size from a few micrometers to a few millimeters [11,20] and thus the effect of gravity is neglected (i.e., $\mathbf{F}_b = \mathbf{0}$). $\mathbf{x} = (x, y)$ is the position vector and $\mathbf{x}_f$ indicates the position of the interface.

Equations (4)–(6) are discretized by a finite difference method and the discretized equations are solved on the uniformly distributed, staggered background grid. A second-order predictor-corrector scheme is used to integrating the equations in time. Such discretization and integration are to give the highest possible accuracy [24]. We use the location of the inner droplet to construct the indicator functions to specify three fluids and their fluid properties at every location in the domain [10].

The boundary conditions are as follows. At the left and right boundaries, we set a periodic condition. At the top boundary, $\mathbf{u} = (U, 0)$ is specified and $\mathbf{u} = (-U, 0)$ is set at the bottom boundary. Accordingly, a shear rate γ is created:

$$\gamma = 2U/H, \quad (8)$$

where H is the height of the domain and is chosen as $6R_2$. The domain width is denoted by W and equal to $24R_2$ (Figure 1) [10]. The dimensionless time is $\tau = \gamma t$.

When the droplets move, the length of interface segments is changed in time due to the movement of the interface points (Equation (3)) but it is always in the range of $0.2\,h$–$0.8\,h$ by deleting or adding front elements, where h is the grid spacing of the background grid [24]. To handle the merging of two droplets, we calculate the distance from one segment of one droplet interface to another segment of the other droplet interface. As this distance is smaller than $0.5\,h$, the droplets perform merging. This coalescence technique has been widely used in front-tracking-based simulations [24]. Like other front-capturing techniques, for example, the level set method [26] and the volume of fluid method [27], the coalescence is dependent on the grid spacing. However, we can easily add a physics-based coalescence treatment to our method but it is not considered in this study. The method was implemented in Fortran (i.e., an in-house serial code) originally developed by Unverdi and Tryggvason [28]. The code was run on a 3.6 GHz Intel Core i9-9900 K workstation. The CPU time, for example, for a typical case, using a 1536×384 grid resolution (discussed below) was about fifty-three hours.

Figure 2 presents the results of our grid convergence study for a merging mode using four grid resolutions 0512×128, 1024×256, 1536×384 and 2048×512. The parameters defined below are $Re = 1.58$, $Ca = 0.01$, $R_{12} = 0.65$, $\sigma_{12} = 1.0$, $\Delta x_{o0}/R_2 = 3.0$, $\Delta y_{o0}/R_2 = 0.6$, $\varepsilon_{x0} = \varepsilon_{y0} = 0.0$. This merging case is selected for the grid study because the merging mode is sensitive to the grid resolution. The shapes of the droplets plotted at $\tau = 2.0$, 4.0 and 12.0 are compared among four grids. Figure 2 indicates that no difference in the droplet shape is available before merging ($\tau = 2.0$ and 4.0). However, because of merging at different resolutions, the shapes of the droplets are different after merging. The most difference is for the inner droplet and the coarsest grid, while we see almost the same results for the outer droplet shape with a little difference in the inner droplet shape when 1536×384 and 2048×512 were used. Accordingly, we believe that the grid resolution of 1536×384 used for the computational results presented below is acceptable. The grid independence study for a passing mode with a higher Ca (i.e., $Ca = 0.1$) was described in Reference [10]. It is noting that the grid resolution used in the present study is finer than that in our previous [10]. The method accuracy was also confirmed in our previous work [10] as illustrated in Figure 3. For this comparison, the values of the Capillary and Reynolds numbers are 0.25 and 1.0. Three fluids of the compound droplets are identical. Initially, the droplets are concentric. The inner-to-outer radius ratios R_{12} (defined below) of 0.5 is computed and

the steady-state shape of the droplet and its outer deformation parameter are compared with those of Hua et al. [16]. The comparison indicates clearly that the method predicts very well the deformation of the compound droplets in the simple shear flow. A more detailed description of this validation can be found in Reference [10]. More comparisons supporting the method accuracy can be found in References [12,13,24,29].

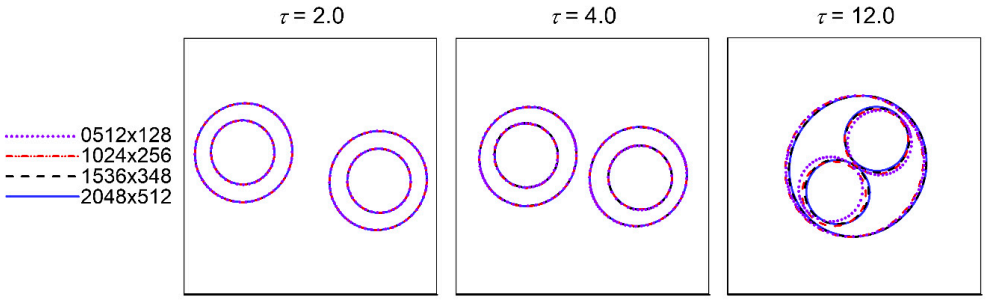

Figure 2. The grid refinement study for a merging case with $Ca = 0.01$, $\varepsilon_{x0} = 0.1$ and $\varepsilon_{y0} = 0.0$. The other parameters are shown in the text.

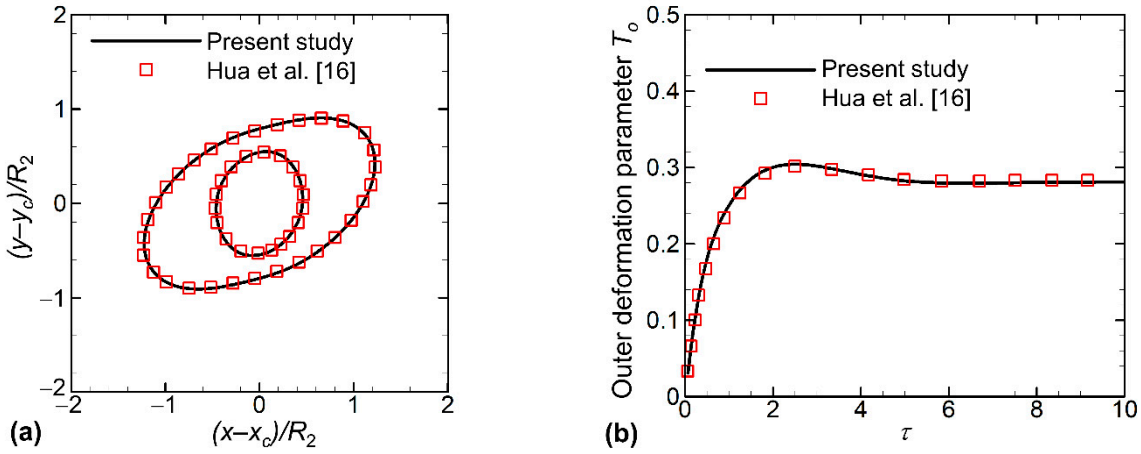

Figure 3. The finite deformation of an initially concentric single-core compound droplet with $R_{12} = 0.5$ in the simple shear flow and the results are compared with Hua et al. [16]: (**a**) the steady-state droplet shape and (**b**) the temporal variation of the deformation parameter of the outer droplet. (x_c, y_c) denote the coordinates of the domain center. Other parameters are shown in the text.

3. Results and Discussion

3.1. Colliding Modes

Our previous works [10,12] assumed that the compound droplet is concentric at the beginning of computations and the following parameters govern the dynamics of the problem:

$$Re = \frac{\rho_3 \gamma R_2^2}{\mu_3}, Ca = \frac{\mu_3 \gamma R_2}{\sigma_2} \tag{9}$$

$$R_{12} = \frac{R_1}{R_2}, \Delta x_{o0}, \Delta y_{o0} \tag{10}$$

$$\sigma_{12} = \frac{\sigma_1}{\sigma_2}, \rho_{13} = \frac{\rho_1}{\rho_3}, \rho_{23} = \frac{\rho_2}{\rho_3}, \mu_{13} = \frac{\mu_1}{\mu_3}, \mu_{23} = \frac{\mu_2}{\mu_3}. \tag{11}$$

Here, Re and Ca are the Reynolds and Capillary numbers. R_{12}, Δx_{o0} and Δy_{o0} are respectively the droplet radius ratio, the initial distances between two outer droplets (calculated from their centers

of mass, Figure 1) in the x- and y-directions. σ_{12} is the interfacial tension ratio of the inner to outer droplets. Accordingly, we also use these parameters in the present study. However, in this study, we pay attention to the effects of the compound droplet eccentricity on collision modes and thus ε_{x0} and ε_{y0} are addressed and the focus of this study. Accordingly, except for ε_{x0} and ε_{y0} and Ca, the other parameters are kept fixed: Re = 1.58, R_{12} = 0.65, σ_{12} = 1.0, $\Delta x_{o0}/R_2$ = 3.0, $\Delta y_{o0}/R_2$ = 0.6 with the density and viscosity ratios set to unity. These values are based on our previous works [10,12] to figure out various modes of collisions as shown below.

Figure 4 shows the different modes of collisions including the merging mode (Ca = 0.01, Figure 4a), the reversing mode (Ca = 0.04, Figure 4b) and the passing-over mode (Ca = 0.16, Figure 4c) [10]. The parameters for these behaviors are ε_{x0} = 0.1 and ε_{y0} = 0.0. As illustrated, when two droplets come into contact, the droplets are almost circular for the small Capillary numbers (Ca = 0.01 and 0.04) but much deformed in the case of the high Ca (Ca = 0.16). Accordingly, when contacting (the frames in the middle row of Figure 4), more circular droplets result in a merging mode while more deformed droplets induce a passing-over mode. The reason is that, for the high Ca, the pressure of the squeezed fluid film in the region between two droplets is strong enough (as compared to the pressure inside the droplets) to prevent the droplets from merging [10]. In contrast, in the case of Ca = 0.01 corresponding to the interfacial tension force dominating over the viscous force, no fluid film in between the droplets is generated and thus the droplets merge easily to produce a larger compound droplet when they come very close to each other (Figure 4a). The reversing mode (Figure 4b) is dominant when there exists a gap between them during the droplet 1 moving downward (and droplet 2 moving upward). A better understanding can be found in the animations of these collision modes provided in the Supplementary Materials.

The trajectories of the outer droplet 1 (the droplet on the left of the domain at the beginning of the computation) in three cases are illustrated in Figure 5b with its corresponding deformation parameters T_o (Figure 5a) for the outer interface (i.e., outer deformation parameter), defined as:

$$T_o = \frac{L_o - D_o}{L_o + D_o}, \tag{12}$$

where L_o and D_o are respectively the maximum and minimum distances from the center of mass to a point on the outer interface. From the beginning, the droplet 1 becomes more deformed as it moves to the right. Before contacting with the other on the right side (i.e., compound droplet 2), the droplet 1 goes down. In the case of merging, the resulting droplet stays at the center. In the case of reversing, the deformation of the droplet decreases a little when it moves to the center. It then experiences more deformation when going back to the left. The most deformed droplet corresponds to Ca = 0.16 for the passing-over mode because of a low interfacial tension force as compared to the viscous force. The droplets have the maximum deformation at the beginning of the contacting stage because of the presence of the fluid film in between them. Their deformation is then decreased when they are about to split away [10,20]. When two droplets are far away from each other, they gradually reach a less deformed shape, resulting in a decrease in the deformation parameter. The reason for this decrease is that when moving to the other side of the domain (after contacting) the droplets are driven to the center plane where the effect of the shear rate on the droplets is minor and thus the interfacial tension force makes the droplets less deformed.

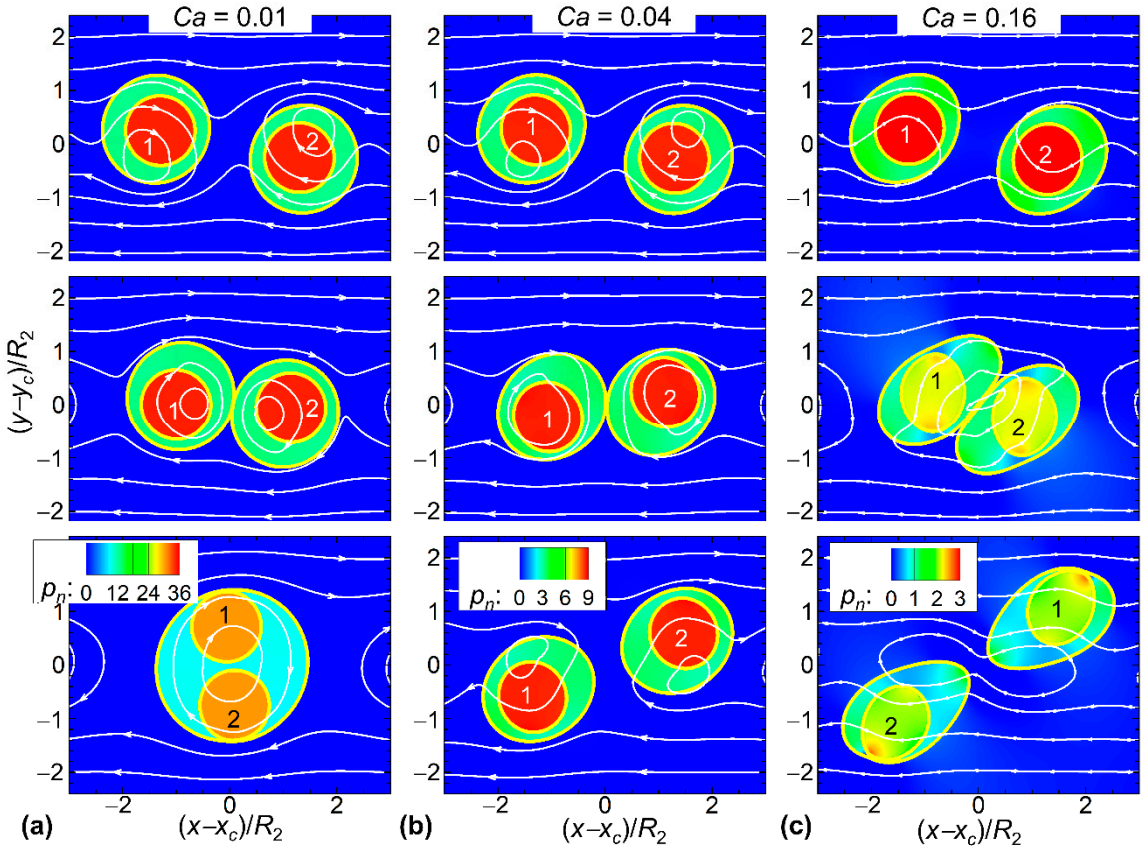

Figure 4. Three collision modes of two eccentric compound droplets: (**a**) merging, (**b**) reversing and (**c**) passing-over. In (**a**)–(**c**), from the top to the bottom, the corresponding time is τ = 2.0 (before contacting), 9.2 (in contact) and 14.0 (after contacting). ε_{x0} = 0.1 and ε_{y0} = 0.0. Color shows the normalized pressure field $p_n = p/(0.5\rho_3 U^2)$. The animations are available in the Supplementary Materials for better understanding of these modes (Video S1: merging mode, Video S2: reversing mode and Video S3: passing-over mode).

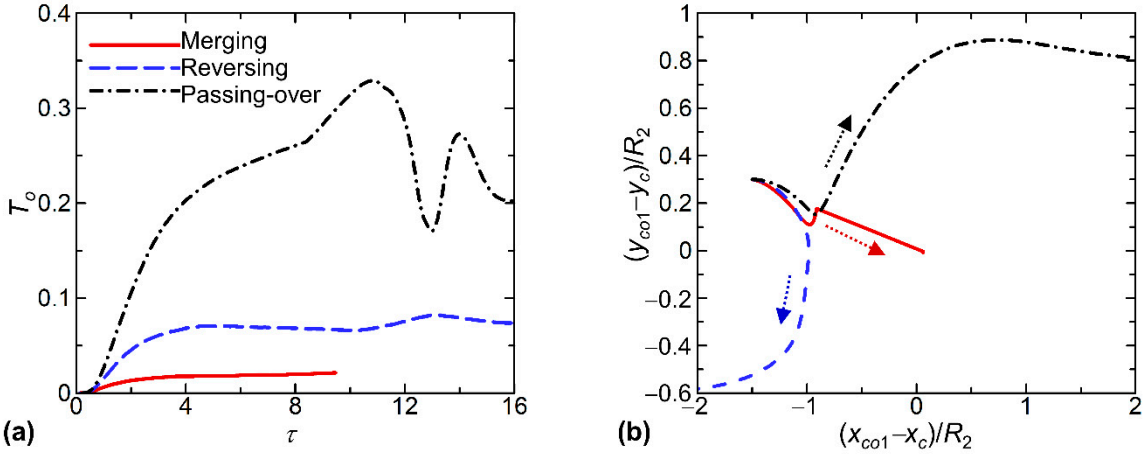

Figure 5. (**a**) The deformation parameter T_o of the outer droplet of the droplet 1 with (**b**) its trajectory in three modes shown in Figure 4. The line definitions in (**a**) also apply for (**b**). (x_{co1}, y_{co1}) are the center of mass of the outer droplet 1. The arrows show the movement directions of the droplet.

3.2. *Effect of the Horizontal and Vertical Eccentricities*

Figure 6 shows the spatiotemporal motion of two droplets in colliding for different horizontal eccentricity $\varepsilon_{x0}/R_2 = -0.1$ (top), 0.2 (middle) and 0.3 (bottom). The other parameters are $Ca = 0.02$ and $\varepsilon_{y0}/R_2 = 0.0$. We can see that when the compound droplets come in contact with one another, the inner droplet circulates in each outer droplet. In the case of $\varepsilon_{x0}/R_2 = -0.1$ (Figure 6a), initially two inner droplets, in terms of the center of mass, are further than the outer droplets. Then, during coming into contact with each other, the inner droplet 1 tends to move upwards while the other inner droplet moves downwards (at $\tau = 4$). Accordingly, when the droplets are in contact, two inner droplets at the other ends (at $\tau = 8$) help them to pass over one another at a later time (at $\tau = 12$). For the other cases, the inner droplets are closer than the outer droplets (Figure 6b,c) and thus when the droplets are in contact, the inner droplet 1 intends to pull the outer droplet 1 downward while the outer droplet 2 is pulled upward. In the case of the closet one ($\varepsilon_{x0}/R_2 = 0.3$), the inner droplets support the droplet merging while they result in a reversing mode for the remainder. Accordingly, for $Ca = 0.02$, increasing the horizontal distance between the inner droplets, the outer droplets change from the passing-over mode (Figure 6b) to the merging over mode (Figure 6c).

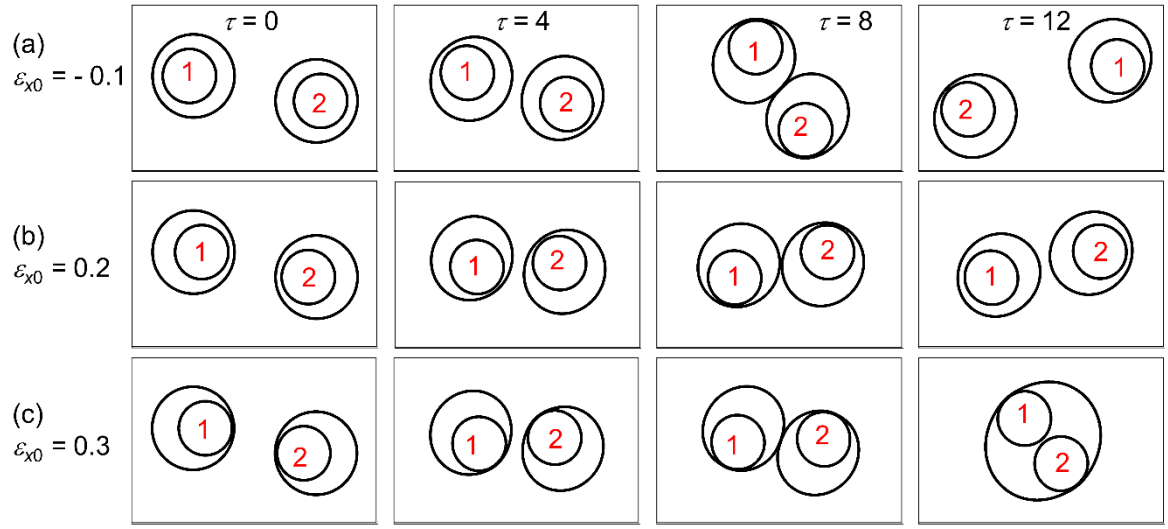

Figure 6. The effect of the horizontal eccentricity on the colliding behaviors of the compound droplets: (**a**) passing-over, (**b**) reversing and (**c**) merging. Other parameters are shown in the text.

Figure 7 shows the droplet profiles at different moments of collisions with different vertical eccentricities $\varepsilon_{y0}/R_2 = -0.2$ (top), 0.1 (middle) and 0.3 (bottom). The other parameters are $Ca = 0.02$ and $\varepsilon_{x0}/R_2 = 0.0$. As previously mentioned, when the droplet 1 moves to the right to collide with the droplet 2, its inner droplet goes around in a clockwise direction. Hence, for $\varepsilon_{y0}/R_2 = -0.2$ and 0.1, the inner droplet 1 in the upper half of the compound droplet 1 tends to push its outer droplet upward during the colliding stage ($\tau = 8.0$). Thereby, the compound droplets in these cases pass over each other (Figure 7a,b). In contrast, in the case that two inner droplets are initially at the furthest distance (Figure 7c), the inner droplet 1 is in the lower half of its outer droplet when two compound droplets are in contact ($\tau = 8.0$). Accordingly, the inner droplet 1 pulls the compound droplet 1 downward and promotes the droplet merging.

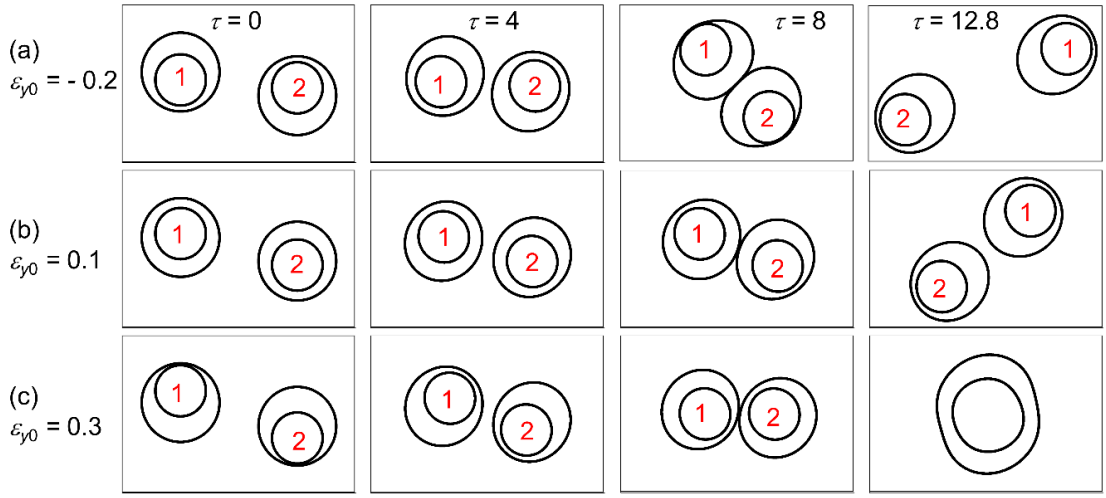

Figure 7. The effect of the vertical eccentricity on the colliding behaviors of the compound droplets: (**a**,**b**) passing-over and (**c**) merging. Other parameters are shown in the text.

Figure 8 shows the movements of the center of mass of the inner droplet 1 about the center of mass of its outer droplet for the cases shown in Figures 6 and 7. This figure illustrates clearly that the inner droplet 1 circulates around the center of the outer droplet 1. As mentioned above, in the passing-over cases [$\varepsilon_{x0}/R_2 = -0.1$ (Figure 6a) and $\varepsilon_{y0}/R_2 = -0.2$ and 0.1 (Figure 7a,b)] the inner droplet is moving upward at the stage of contacting (τ = 8.0 for $\varepsilon_{x0}/R_2 = -0.1$ and τ = 8.0 for $\varepsilon_{y0}/R_2 = -0.2$ and 0.1) while it is moving downward for the other cases. The reversing mode appears when the outer droplets are not so close to one another (τ = 8.0 in Figure 6b). When the outer droplets overlap a bit (in the horizontal direction) (τ = 8.0 in Figure 6c or τ = 8.0 in Figure 7c), they merge at a later time. We also observe such rotations of the inner droplet 1 about the center of its enclosing droplet for Ca = 0.01 and Ca = 0.16, as shown in Figure 9. However, as aforementioned, a very small Ca (Ca = 0.01) results in a merging mode while a high Ca (Ca = 0.16) corresponds to a passing-over mode [10,12]. Thus, when the Capillary number is the dominantly controlling parameter for the formation of the collision modes, the position and the rotation of the inner droplet has almost no impact on the colliding behaviors of two droplets, as illustrated in Figure 9.

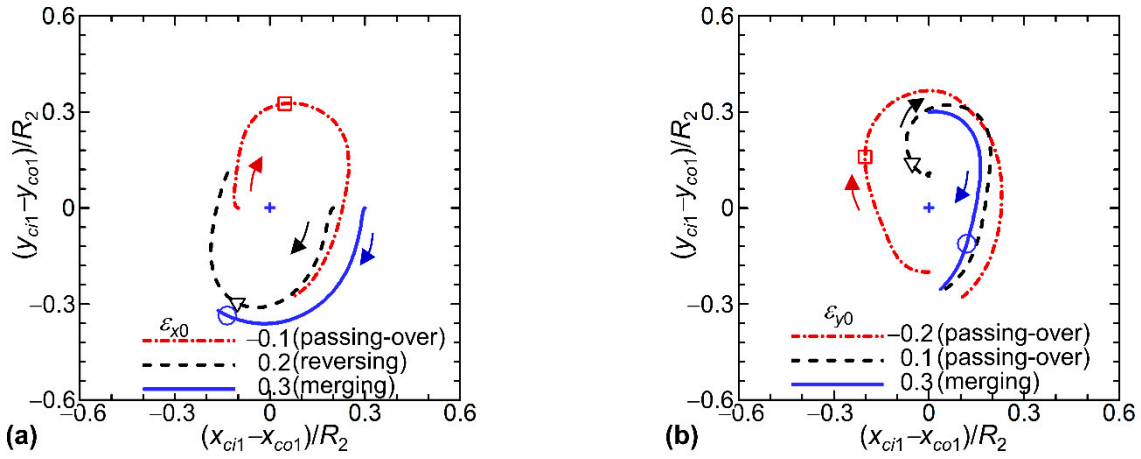

Figure 8. (**a**) The trajectories of the center of mass (x_{ci1}, y_{ci1}) of the inner droplet 1 relative to the center of mass (x_{co1}, y_{co1}) of the outer droplet 1 shown in Figure 6. (**b**) The trajectories of the center of mass (x_{ci1}, y_{ci1}) of the inner droplet 1 relative to the center of mass (x_{co1}, y_{co1}) of the outer droplet 1 shown in Figure 7. The symbols in (**a**) indicate the cases at τ = 8.0 shown in Figure 6, while the symbols in (**b**) indicate the cases at τ = 8.0 shown in Figure 7. The arrows show the movement directions.

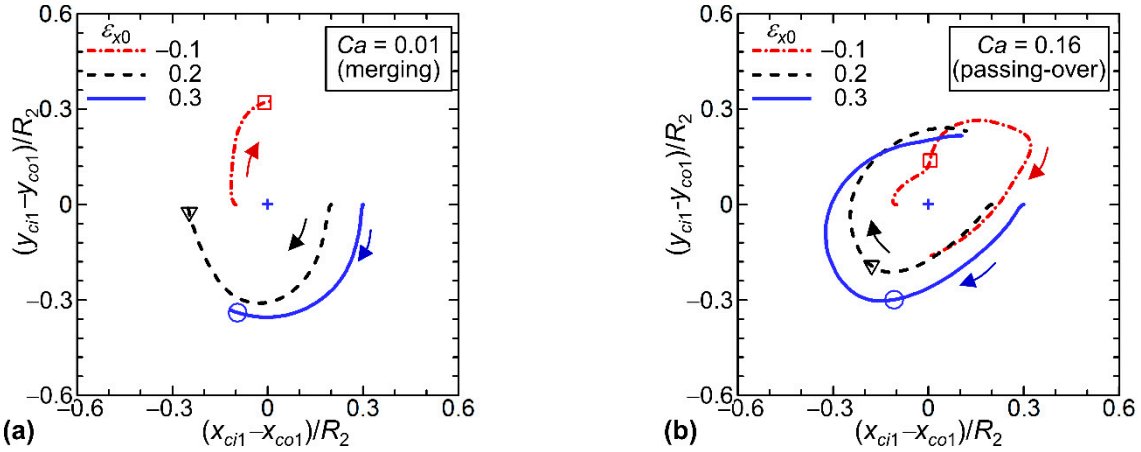

Figure 9. The trajectories of the center of mass (x_{ci1}, y_{ci1}) of the inner droplet 1 relative to the center of mass (x_{co1}, y_{co1}) of the outer droplet 1 for (**a**) Ca = 0.01 (merging modes) and (**b**) Ca = 0.16 (passing-over modes). The symbols indicate the moments of the contacting stage. The arrows show the movement directions.

3.3. Region Diagrams of Colliding Modes

It is evident that the droplet eccentricity has an impact on the colliding behaviors of the compound droplets, for example, for Ca = 0.02. To provide a more complete picture of the colliding behaviors with the presence of the droplet eccentricity, we have performed more simulations with Ca varied in the range of 0.005–0.32. For each value of Ca, we varied ε_{x0}/R_2 (while keeping ε_{y0} = 0.0) and ε_{y0}/R_2 (while keeping ε_{x0} = 0.0) from −0.3 to 0.3 to show the effects of each eccentric factor. As shown in Figure 4, increasing the value of the Capillary number corresponding to decreasing the interfacial tension force and more deformed droplets enhances the passing-over mode [10]. Accordingly, in the region diagrams of Ca versus ε_{x0} and ε_{y0} (Figure 10) two compound droplets pass over each other when the values of the parameters fall within the right side of the diagrams. At a small Ca (i.e., $Ca \leq 0.01$) the merging mode is available for almost all values of ε_{x0} and ε_{y0}. This is understandable since at a small Ca, the interfacial tension force is very dominant over the viscous force and thus the position of the inner droplets has a very minor effect. At a value of Ca in the range of 0.02–0.08, the location of the inner droplet at the beginning of collisions plays a role in the colliding behavior. That is, the collision changes from a passing-over mode to a reversing mode and a merging mode when two inner droplets are closer in the horizontal direction, that is, ε_{x0}/R_2 varying from −0.3 to 0.3 (from the bottom to the top of the diagram, Figure 10a). However, the effects of the vertical eccentricity ε_{y0} are not so dominant as ε_{x0} = 0.0, as shown in Figure 10b. The effects of the combinations of non-zero ε_{x0} and ε_{y0} are shown in Figure 11.

Figure 11 indicates the colliding modes appearing for Ca = 0.01, 0.04 and 0.16 when we varied ε_{y0} in the range of −0.3–0.3 for each ε_{x0} varied in the range of −0.3–0.3. It is clear that at a small Ca (Ca = 0.01) the dominant mode is merging while for Ca = 0.04 and Ca = 0.16 the passing mode occupies almost entire diagrams. The reserving mode occurs only for ε_{x0} = 0.15 with most cases corresponding to $\varepsilon_{y0} \geq 0.0$ (Figure 11a,b). In such colliding cases, the inner droplet 1 behaves similarly to that shown in Figure 6b, in which the inner droplet 1 has a tendency of pulling its enclosing droplet down during the stage of contacting (the dash line in Figure 8a). Figure 11 also confirms that the compound droplet eccentricity has the most influence for the value of the Capillary number in the range of 0.01–0.04.

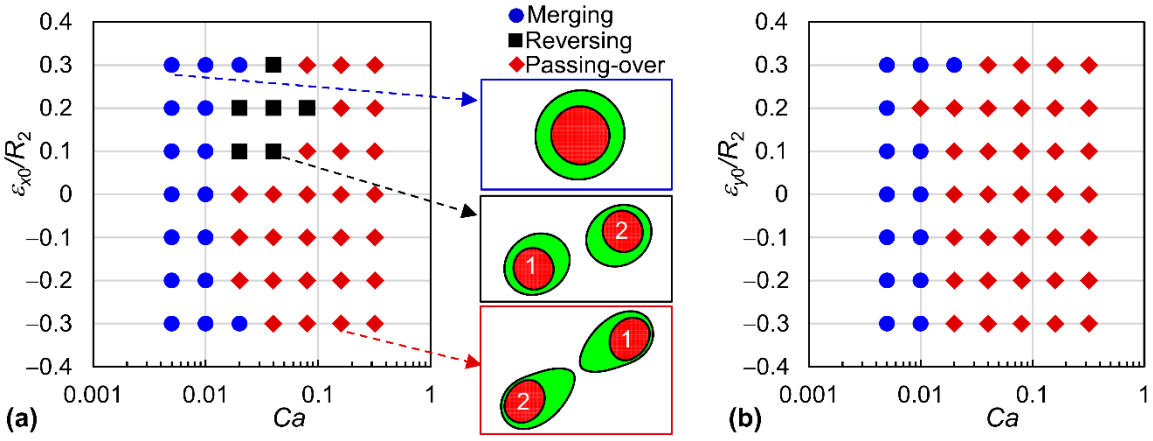

Figure 10. The region diagrams of the colliding modes of two eccentric compound droplets: (**a**) *Ca* versus ε_{x0} (with $\varepsilon_{y0}/R_2 = 0.0$) and (**b**) *Ca* versus ε_{y0} (with $\varepsilon_{x0}/R_2 = 0.0$). Initially, the droplet 1 is on the left and in the upper half of the domain.

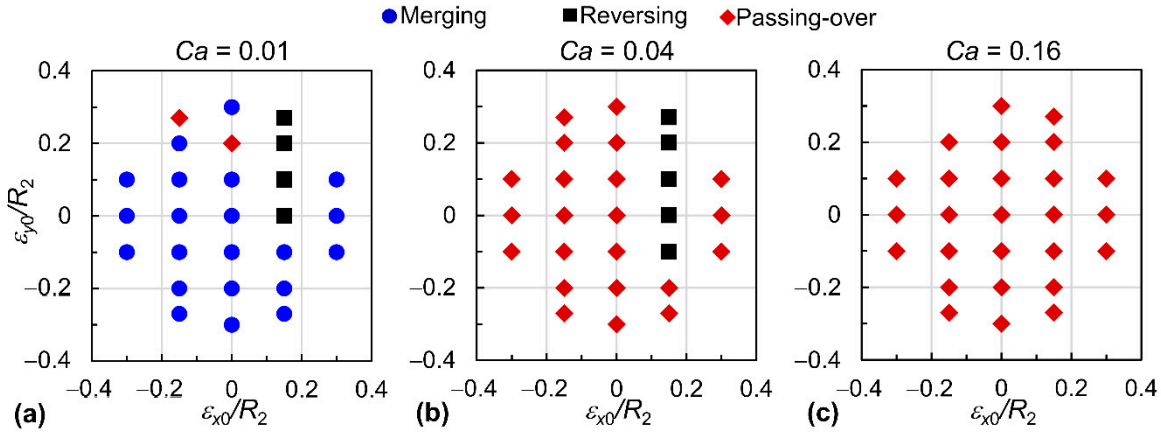

Figure 11. The ε_{x0}-versus-ε_{y0} region diagrams of the colliding modes of two eccentric compound droplets for (**a**) $Ca = 0.01$ and (**b**) $Ca = 0.04$ and (**c**) $Ca = 0.16$. Initially, the droplet 1 is on the left and in the upper half of the domain.

4. Conclusions

We have presented the computational results of two single-core compound droplets colliding in the simple shear flow undergoing the influence of eccentricity. The Capillary number *Ca* is varied in the range of 0.005 to 0.32 with $Re = 1.6$, $R_{12} = 0.65$ and the ratios of material properties set to unity. The eccentricities in terms of ε_{x0} (x direction) and ε_{y0} (y direction) are varied from −0.3 to 0.3. The results are three modes of collisions (merging, reversing and passing-over) recognized. The collision modes for $Ca \leq 0.01$ resulting in the merging mode and $Ca \geq 0.16$ leading to the formation of the passing-over mode are almost independent of the location of the inner droplets. In contrast, when the value of *Ca* is varied from 0.02 to 0.16, the eccentricity becomes important and affects the modes of collisions. Particularly, ε_{x0} varying from −0.3 to 0.3 can cause the collision behavior to change from a passing-over mode to a reversing mode and ends at a merging mode, for example, for $Ca = 0.02$ with $\varepsilon_{y0} = 0.0$. While varying in this range (−0.3–0.3), ε_{y0} induces the transitions just between the merging and reversing modes (e.g., for $Ca = 0.01$ and $\varepsilon_{x0} = 0.15$), or between the passing-over and reversing modes (e.g., for $Ca = 0.04$ and $\varepsilon_{x0} = 0.15$), or between the passing-over and merging modes (e.g., for $Ca = 0.02$ and $\varepsilon_{x0} = 0.0$).

The present study (or our previous work [10]) is limited to two-dimensional results and single-core compound droplets. Accordingly, three-dimensional computations are necessary for more accurate

predictions and to consider the effect of the eccentricity caused by the inner droplet located out of the plane through the centers of two outer droplets. In addition, to find out what will happen when the compound droplets encapsulate many inner droplets.

Supplementary Materials: The following are available online at http://www.mdpi.com/2227-9717/8/5/602/s1, Video S1: a merging mode with $Ca = 0.01$, $\varepsilon_{x0} = 0.1$ and $\varepsilon_{y0} = 0.0$, Video S2: a reversing mode with $Ca = 0.04$, $\varepsilon_{x0} = 0.1$ and $\varepsilon_{y0} = 0.0$, Video S3: a passing-over mode with $Ca = 0.16$, $\varepsilon_{x0} = -0.2$ and $\varepsilon_{y0} = 0.0$.

Author Contributions: Study design, T.V.V.; method modification, T.V.V.; computations, K.P.N. and T.V.V.; data analysis, K.P.N. and T.V.V.; writing the paper, K.P.N. and T.V.V. All authors have read and agreed to the published version of the manuscript.

Funding: This research is funded by Vietnam National Foundation for Science and Technology Development (NAFOSTED) under grant number 107.03-2019.307.

Acknowledgments: The authors are grateful to John C. Wells at Ritsumeikan University, Japan for facilitating computing resources.

Conflicts of Interest: The authors declare no conflict of interest.

References

1. Bazhlekov, I.B.; Shopov, P.J.; Zapryanov, Z.D. Unsteady motion of a type-A compound multiphase drop at moderate reynolds numbers. *J. Colloid Interface Sci.* **1995**, *169*, 1–12. [CrossRef]
2. Zhang, Y.; Chatain, D.; Anna, S.L.; Garoff, S. Stability of a compound sessile drop at the axisymmetric configuration. *J. Colloid Interface Sci.* **2016**, *462*, 88–99. [CrossRef] [PubMed]
3. Teh, S.-Y.; Lin, R.; Hung, L.-H.; Lee, A.P. Droplet microfluidics. *Lab Chip* **2008**, *8*, 198–220. [CrossRef] [PubMed]
4. Vu, T.V.; Wells, J.C.; Takakura, H.; Homma, S.; Tryggvason, G. Numerical calculations of pattern formation of compound drops detaching from a compound jet in a co-flowing immiscible fluid. *J. Chem. Eng. Jpn.* **2012**, *45*, 721–726. [CrossRef]
5. Vu, T.V.; Takakura, H.; Wells, J.C.; Minemoto, T. Breakup modes of a laminar hollow water jet. *J. Vis.* **2011**, *14*, 307–309. [CrossRef]
6. Wang, J.; Liu, J.; Han, J.; Guan, J. Rheology investigation of the globule of multiple emulsions with complex internal structures through a boundary element method. *Chem. Eng. Sci.* **2013**, *96*, 87–97. [CrossRef]
7. Lamba, H.; Sathish, K.; Sabikhi, L. Double Emulsions: Emerging Delivery System for Plant Bioactives. *Food Bioprocess Technol.* **2015**, *8*, 709–728. [CrossRef]
8. McClements, D.J. Advances in fabrication of emulsions with enhanced functionality using structural design principles. *Curr. Opin. Colloid Interface Sci.* **2012**, *17*, 235–245. [CrossRef]
9. Vu, T.V.; Takakura, H.; Wells, J.C.; Minemoto, T. Production of hollow spheres of eutectic tin-lead solder through a coaxial nozzle. *J. Solid Mech. Mater. Eng.* **2010**, *4*, 1530–1538. [CrossRef]
10. Vu, T.V. Parametric study of the collision modes of compound droplets in simple shear flow. *Int. J. Heat Mass Transf.* **2019**, *79*, 108470. [CrossRef]
11. Liu, X.; Wang, C.; Zhao, Y.; Chen, Y. Shear-driven two colliding motions of binary double emulsion droplets. *Int. J. Heat Mass Transf.* **2018**, *121*, 377–389. [CrossRef]
12. Vu, T.V.; Vu, L.V.; Pham, B.D.; Luu, Q.H. Numerical investigation of dynamic behavior of a compound drop in shear flow. *J. Mech. Sci. Technol.* **2018**, *32*, 2111–2117. [CrossRef]
13. Vu, T.-V.; Vu, T.V.; Bui, D.T. Numerical study of deformation and breakup of a multi-core compound droplet in simple shear flow. *Int. J. Heat Mass Transf.* **2019**, *131*, 1083–1094. [CrossRef]
14. Stone, H.A. Dynamics of drop deformation and breakup in viscous fluids. *Annu. Rev. Fluid Mech.* **1994**, *26*, 65–102. [CrossRef]
15. Chen, Y.; Liu, X.; Shi, M. Hydrodynamics of double emulsion droplet in shear flow. *Appl. Phys. Lett.* **2013**, *102*, 051609. [CrossRef]
16. Hua, H.; Shin, J.; Kim, J. Dynamics of a compound droplet in shear flow. *Int. J. Heat Fluid Flow* **2014**, *50*, 63–71. [CrossRef]
17. Luo, Z.Y.; He, L.; Bai, B.F. Deformation of spherical compound capsules in simple shear flow. *J. Fluid Mech.* **2015**, *775*, 77–104. [CrossRef]

18. Qu, X.; Wang, Y. Dynamics of concentric and eccentric compound droplets suspended in extensional flows. *Phys. Fluids* **2012**, *24*, 123302. [CrossRef]
19. Wang, J.; Xu, S.; Huang, Y.; Guan, J. Mechanical mechanisms of the directional shift and inverse of the eccentric compound droplet. *Phys. Fluids* **2018**, *30*, 042005. [CrossRef]
20. Liu, X.; Wang, C.; Zhao, Y.; Chen, Y. Passing-over motion during binary collision between double emulsion droplets under shear. *Chem. Eng. Sci.* **2018**, *183*, 215–222. [CrossRef]
21. Abate, A.R.; Weitz, D.A. High-order multiple emulsions formed in poly (dimethylsiloxane) microfluidics. *Small* **2009**, *5*, 2030–2032. [CrossRef]
22. Kim, S.-H.; Kim, B. Controlled Formation of Double-Emulsion Drops in Sudden Expansion Channels. *J. Colloid Interface Sci.* **2014**, *415*, 26–31. [CrossRef]
23. Shah, R.K.; Shum, H.C.; Rowat, A.C.; Lee, D.; Agresti, J.J.; Utada, A.S.; Chu, L.-Y.; Kim, J.-W.; Fernandez-Nieves, A.; Martinez, C.J.; et al. Designer emulsions using microfluidics. *Mater. Today* **2008**, *11*, 18–27. [CrossRef]
24. Tryggvason, G.; Bunner, B.; Esmaeeli, A.; Juric, D.; Al-Rawahi, N.; Tauber, W.; Han, J.; Nas, S.; Jan, Y.-J. A front-tracking method for the computations of multiphase flow. *J. Comput. Phys.* **2001**, *169*, 708–759. [CrossRef]
25. Vu, T.V.; Homma, S.; Wells, J.C.; Takakura, H.; Tryggvason, G. Numerical simulation of formation and breakup of a three-fluid compound jet. *J. Fluid. Sci. Technol.* **2011**, *6*, 252–263. [CrossRef]
26. Sussman, M.; Smereka, P.; Osher, S. A Level Set Approach for Computing Solutions to Incompressible Two-Phase Flow. *J. Comput. Phys.* **1994**, *114*, 146–159. [CrossRef]
27. Hirt, C.W.; Nichols, B.D. Volume of fluid (VOF) method for the dynamics of free boundaries. *J. Comput. Phys.* **1981**, *39*, 201–225. [CrossRef]
28. Unverdi, S.O.; Tryggvason, G. A front-tracking method for viscous, incompressible, multi-fluid flows. *J. Comput. Phys.* **1992**, *100*, 25–37. [CrossRef]
29. Vu, T.-V.; Vu, T.V.; Nguyen, C.T.; Pham, P.H. Deformation and breakup of a double-core compound droplet in an axisymmetric channel. *Int. J. Heat Mass Transf.* **2019**, *135*, 796–810. [CrossRef]

© 2020 by the authors. Licensee MDPI, Basel, Switzerland. This article is an open access article distributed under the terms and conditions of the Creative Commons Attribution (CC BY) license (http://creativecommons.org/licenses/by/4.0/).